Proceedings of the ASME/JSME 2011 8th Thermal Engineering Joint Conference
AJTEC2011
March 13-17, 2011, Honolulu, Hawaii, USA

AJTEC2011-44551

HEAT TRANSFER AND PRESSURE DROP DURING CONDENSATION OF R-134A INSIDE PARALLEL MICROCHANNELS

Gil Goss Júnior[1], Stefano Frasson Macarini[2], Júlio César Passos[3]
LEPTEN/Boiling
Department of Mechanical Engineering
Federal University of Santa Catarina
Florianópolis, Santa Catarina, Brazil
[1]goss@lepten.ufsc.br; [3]tefinh0@gmail.com; [2]jpassos@emc.ufsc.br

ABSTRACT

In this study the pressure drop and local heat transfer coefficient were investigated experimentally during the convective condensation of R-134a inside eight round (D= 0.8 mm) horizontal and parallel microchannels. The test conditions included mass velocity and pressure ranges of 57 to 125 kg.m^{-2}s^{-1} and 6.8 to 11.2 bar, respectively. The experimental results are compared with correlations and semi-empirical models described in the literature.

NOMENCLATURE

A	surface area (m^2)
Co	confinement number (-)
D	diameter (m)
f	friction factor (-)
g	acceleration due to gravity (m.s^{-2})
G	mass velocity (kg.m^{-2}s^{-1})
h	heat transfer coefficient (W.m^{-2}K^{-1})
K	friction coefficient (-)
L	length (m)
m	mass flow rate (kg.s^{-1})
p	pressure (bar)
Q	power (W)
q''	heat flux (W.m^{-2})
T	temperature (K)
x	vapor quality (-)
ΔP	pressure drop (Pa)
z	location (mm)

Greek symbols:

α	void fraction (-)
ϕ	multiplier (-)
γ_{exp}	expansion area ratio (-)
μ	dynamic viscosity (kg.m^{-1}s^{-1})
ρ	density (kg.m^{-3})
σ	surface tension (N.m^{-1})
Ψ_S	non dimensional parameter (-)

Subscripts:

exp	experimental
de	deceleration
c	cold
ch	channel
f	friction
g	vapor phase
h	hydraulic/ hot
i	contraction
in	inlet
l	liquid phase
mani	manifold
o	expansion
tot,ch	total of channels
tp	two-phase
w	wall

INTRODUCTION

Interest in studying two-phase flow in microchannels has increased enormously in the last decade. This has occurred as a consequence of the need to increase the effectiveness of heat exchangers, due to the use of more compact systems, and to reduce the cost of materials and the quantity of refrigerant fluids used.

One consequence of the miniaturization of condensers in air-cooled refrigeration systems, for example, is an increase in the COP caused by a decrease in the pressure drop on the air

Copyright © 2011 by ASME

side, and an increase in the heat transfer coefficient on the refrigerant side. However, it can also lead to an increase in the pressure drop in the refrigerant flow.

Microcondensers are already used in several cooling and refrigeration processes, such as mini heat pipes and compact heat exchangers in the electronics industry, for thermal control in satellites; and in compact air conditioning - both residential and automotive. The latter has been making use of microchannels with $0.5 < D_h < 1.5$ mm [1] for nearly 20 years.

On the other hand, our understanding of the phenomena involving phase change in microgeometries is still in the initial stage, and thus the design of compact heat exchangers still represents a considerable challenge to industry. This is evidenced by the different results found by authors for the heat transfer and pressure drop.

The primary issue regarding studies on two-phase flow in small diameters is related to the transition between macro and microchannels. The main reason for this is that the physics mechanisms are very different when the diameter is reduced to a few millimeters. In [2-4] it is shown that the transitions between flow patterns are not the same for condensation in micro and macrochannels. According to the cited authors, the influence of the forces present during the flow differs. In microscale, the shear and surface tension forces are more important than the gravitational ones, and the opposite occurs when the diameter is larger.

However, Matkovic *et al.* [1] compared their results obtained for heat transfer and pressure drop using R-134a and R32 flowing in 0.96 mm circular channels with correlations proposed for conventional channels. Their results showed no significant discrepancies between experimental and theoretical results.

It is important to note that a transition value between macro and microchannels does not exist. Some authors have proposed different ways to establish this transition, but there is no consensus among authors on a single method. The best criteria proposed are probably those based on physics parameters, like the confinement number (*Co*). This factor, shown in Eqn. (1), is defined as the ratio between the capillary length and hydraulic diameter of the channel.

$$Co = \sqrt{\frac{\sigma}{D_h^2\left[g\left(\rho_l - \rho_v\right)\right]}} \tag{1}$$

where σ, ρ_l, ρ_v, g and D_h represent the surface tension ($N.m^{-1}$), liquid and vapor density ($kg.m^{-3}$), acceleration due to gravity ($m.s^{-2}$) and hydraulic diameter (m), respectively.

Kew and Cornwell [5] proposed that the transition occurs for $Co = 0.5$. In other words, $Co>0.5$ indicates a microchannel and $Co< 0.5$ a macrochannel.

Moreover, the cross-section of the channel influences the heat transfer and pressure drop. Du and Zhao [6] showed that the condensation heat transfer coefficient in rectangular channels is larger than that for circular ducts with the same hydraulic diameter. This is caused by meniscus formation in the corners of non-circular channels.

Ribatski *et al.* [7] tested twelve pressure drop correlations developed for macro- and micro-scale with more than 900 experimental data points for both diabatic and adiabatic flows, for $23<G<6000$ $kg.m^{-2}s^{-1}$, and they concluded that the effect of tube diameter on the pressure drop and flow pattern should be investigated further.

Coleman and Garimella [2,3] performed several experiments on flow visualization for adiabatic air-water flow and R-134a condensing in square horizontal microchannels with 1 mm $<D_h<4.91$ mm. They observed that the hydraulic diameter has a substantial effect on the flow patterns and transitions. However, the tube shape had only a slight influence on the flow pattern. The same authors proposed different condensation flow regime maps for D_h = 1, 2, 3 and 4 mm. For $G>150$ $kg.m^{-2}s^{-1}$, they observed annular, wavy, intermittent (slug, plug) and dispersed flow. As D_h decreases, the annular regime is enhanced, and the wavy regime decreases in size. For 1-mm tubes, the wavy regime completely disappears, confirming that the gravitational force diminishes in microchannels.

Baird *et al.* [8] studied condensation of HCFC-123 and R11 in tubes with diameters of 0.92 and 1.95 mm for a range of mass velocities (70–600 $kg.m^{-2}s^{-1}$), heat fluxes (15–110 kWm^{-2}) and pressures (1.2-4.1 bar). They found that the heat transfer coefficient increased with increasing mass velocity, vapor quality and heat flux (mainly for high vapor qualities). A rise in pressure caused the opposite effect on *h*.

Yan and Lin [9] measured the experimental heat transfer coefficient and pressure drop inside horizontal circular channels (D=2.0 mm) for condensation of R-134a, at $100<G<200$ $kg.m^{-2}s^{-1}$. They observed that the pressure drop increases with vapor quality (mainly for lower saturation temperature) and with G (for high vapor qualities). The authors proposed correlations for friction factor and heat transfer coefficient, which are tested in this study.

Some models and correlations to predict the heat transfer coefficient, pressure drop and flow pattern maps for convective condensation in microchannels have been proposed, mainly for $D_h > 1$ mm. However, they showed large discrepancies even when they were used under similar microchannel conditions as those under which the equations where developed.

The differences between these results occur for two reasons in relation to the heat transfer coefficient: the first is that the available experimental data is very limited; and the second is that most of the data has a high uncertainty level because it is based on the "Wilson plot" technique and/or overall measurement of the subtracted thermal resistances [10].

Most of the correlations proposed to predict the pressure drop during condensation in microchannels are based on modifications from the Lockhart and Martinelli [11], Chisholm [12] and Friedel [13] correlations, which were proposed for conventional diameters, and their results show large deviations compared with experimental data [14].

Copyright © 2011 by ASME

The wide applicability of microcondensers combined with the relative lack of knowledge on the phenomena occurring in microgeometries and the relatively weak prediction capacity in terms of flow behavior, leads to a need to develop new studies on convective condensation in microchannels, mainly in submillimeter geometries, since most studies in this area are based on $D_h > 1$ mm [15].

The objective of this study was to analyze the convective condensation inside eight circular parallel and horizontal microchannels, with 0.8 mm of diameter. The experimental test conditions were: $57<G<125$ kg.m^{-2}s^{-1}; 6.8 bar$<p<$11.2 bar; $20<q''<34$ kW.m^{-2}. The experimental data for the heat transfer coefficient and pressure drop are compared with seven and five empirical correlations proposed in the literature, respectively.

EXPERIMENTAL FACILITIES

The rig operates by producing R-134a vapor in the boiler and channeling it to the test section where different measurements are made. The working fluid is then turned into a liquid in a post condenser and pumped back to the boiler, as shown in Fig. 1.

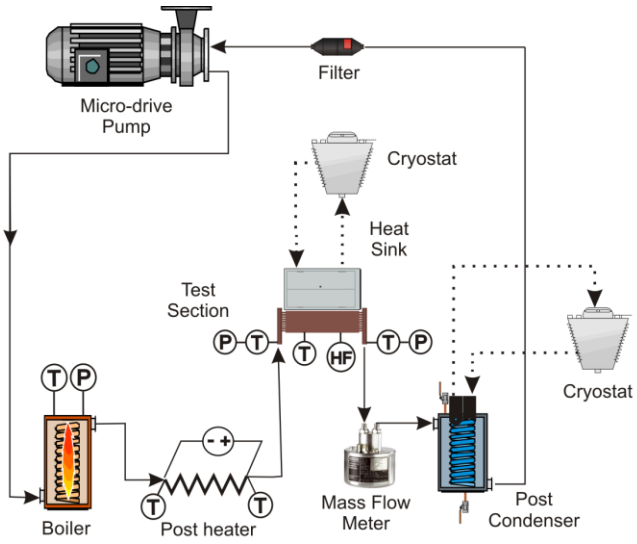

FIGURE 1. EXPERIMENTAL SETUP SCHEME

In the boiler, R-134a is heated to generate saturated vapor (x=1). The temperature and pressure are measured, respectively, by E-type thermocouples (Omega) and pressure transducers (Wärme model WTP-4010). A cartridge-type electrical resistance can be set to deliver power of up to 1000 W to the working fluid, depending on the mass flow required for the test, making it flow through a unidirectional valve to a superheater. The amount of liquid inside the boiler is monitored and when the level is low a sensor triggers the pump, supplying R-134a.

Prior to flowing through the test section, the working fluid passes through a post heater which was turned off during the present experimental analysis. The pressure drop during the flow inside the post heater can be considered negligible. The heat loss across the post heater wall causes a reduction in the vapor quality of less than 3%, for the worst case.

The saturated vapor reaches the test section, first arriving at a manifold, and then flowing inside 8 copper microchannels with D = 0.8 mm each and with 105 mm of length. The channels are assembled under a copper plate, with 3 mm and 90 mm of thickness and length, respectively, been cooled by 3 Peltier coolers (Danvic) placed above it, as shown in Fig. 2.

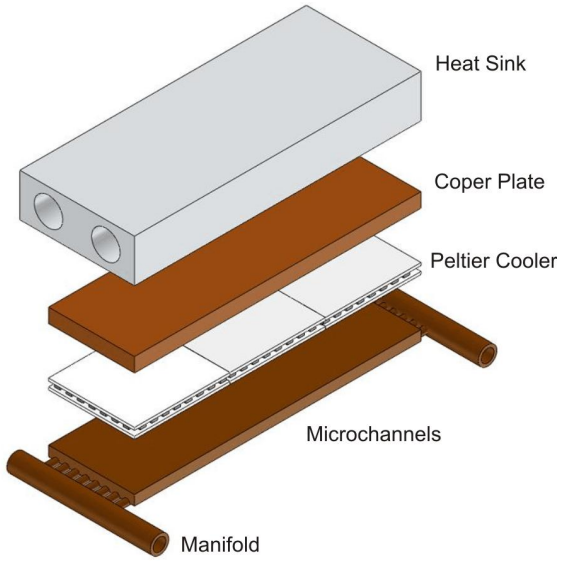

FIGURE 2. TEST SECTION EXPLODED VIEW

Each cooler has 30 x 30 mm^2 and both a cold and a hot side. The rig was assembled in such a way that the cold side is in contact with the test section, and the hot side is cooled by an aluminum heat sink through which an ethylene-glycol and water mixture flows. The coolers can be supplied with a maximum electrical current of 10 A.

Pressure is measured by absolute (at the inlet manifold) and differential (between two manifolds) pressure transducers. Temperature is measured by thermocouples at both the entrance and exit manifolds, as well as at 13 different points on the copper plate, as shown in Fig. 3.

A mixture of vapor and liquid leaves the test section, passes through a mass flow meter and reaches a post condenser, which uses water from a cold bath to totally condense the working fluid. The flow then reaches a filter to remove small particles and avoid problems occurring in the pump. The micropump is a magnetic-drive type (Liquiflo), which operates with a maximum flow rate of 1.83 l/min and sends the R-134a back to the boiler.

Copyright © 2011 by ASME

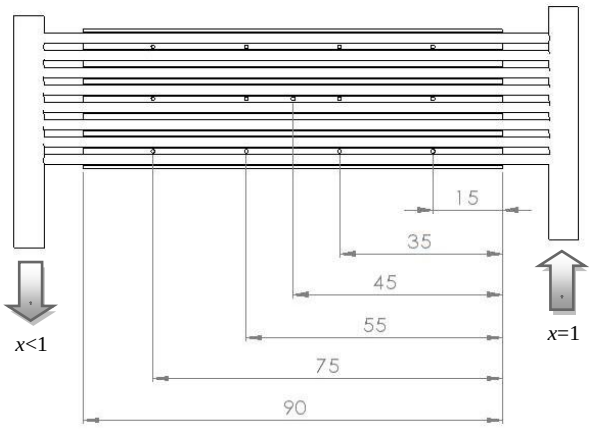

FIGURE 3. LOCATIONS OF THERMOCOUPLES IN THE TEST SECTION (in mm)

Each of the three Peltiers is calibrated to allow the calculation of heat flux removed from the fluid. The power removed was found to be a function of the electrical current supplied and the temperatures on both sides of the coolers. This calibration procedure had a maximum uncertainty of 2 W for the heat removed. Fig. 4 shows the curves for one Peltier cooler.

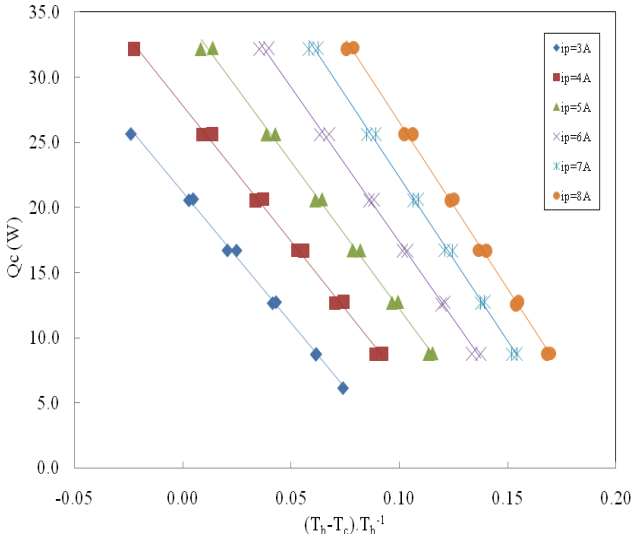

FIGURE 4. CALIBRATION CURVE OF PELTIER COOLER

EXPERIMENTAL PROCEDURE

The voltage in the boiler is set manually using a voltage controller, delivering power to the resistor and heating up the working fluid to a saturated vapor state. The inlet temperature in the test section can be adjusted by changing the power delivered to the superheater. The power of Peltier cooler can also be modified, thus allowing tests to be carried out with different heat fluxes. A needle valve was installed after the test section in an attempt to run tests with different pressures for the same mass velocity, but it did not provide good flux control. Thus, the mass velocity appears to be dependent on the pressure in the boiler. All data were collected via an HP 39470-A data acquisition system, and then visualized and saved onto a microcomputer with LabVIEW software.

DATA REDUCTION

The MATLAB program was used to perform all data treatment. It received the temperature and pressure data collected at the entrance and exit of the test section, and also the heat flux and mass flow rate. The program divides the test section into 100 intervals, performing calculations for pressure, temperature and enthalpy drop for the interval length, and delivering the new data to the subsequent interval. In this way it is possible evaluate conditions like pressure, vapor quality, fluid and wall temperature at each point from the inlet of the test section.

The temperature and pressure at the entrance in the first interval are known (x=1). The program calculates all fluid properties needed for this condition using EES. With the heat flux data, the final enthalpy can be calculated by means of a heat balance. The other property required to define the state at this location is calculated by determining the pressure at each point. This is carried out by a linearization of the pressure drop between the inlet and outlet of the channels. Finally, the mean vapor quality within the interval can be determined and the entrance condition of the subsequent interval is the final condition of the previous.

All calculations are carried out using the mass velocity mean, defined as follows:

$$G = \frac{\dot{m}}{8A_{ch}} \tag{2}$$

where A_{ch} and $\dot{m}$ represent the cross-sectional flow area (m) and the mass flow rate (kg.s^{-1}), respectively.

Pressure drop

The total pressure drop results from a combination of four phenomena at the measurement point (manifold). Apart from the friction, ΔP_f, there is a pressure gain related to the flow deceleration, ΔP_{de}, due to the phase change. The other contributions are due to the fluid contraction, ΔP_i, and expansion, ΔP_o, at the inlet and outlet of the channels. Thus, the experimental pressure drop, ΔP_{exp}, measured comprises:

$$\Delta p_{exp} = \Delta p_f - \Delta p_{de} + \Delta p_i - \Delta p_o \tag{3}$$

Copyright © 2011 by ASME

TABLE 1. CONDITIONS USED TO OBTAIN FRICTIONAL TWO-PHASE PRESSURE DROP CORRELATIONS

Author	D_h (mm)	Fluids	G ($kg.m^{-2}s^{-1}$)
Yan and Lin [9]	2.0	R-134a	100-200
Lockhart and Martinelli [11]	1.5-26	air/benzene,kerosene,water/oils	-
Wilson *et al.* [21]	1.84-7.79	R-134a, R-410a	75-400
Zang and Webb [22]	0.96-6.25	R-12	400-1400
Cavallini *el al.* [23]	1.4	R-134a, R-236ea, R-410a	200-1400

TABLE 2. CONDITIONS USED TO OBTAIN HEAT TRANSFER COEFFICIENT CORRELATIONS

Author	D_h (mm)	Fluids	G ($kg.m^{-2}s^{-1}$)
Yan and Lin [9]	2.0	R-134a	100-200
Traviss *et. al* [20]	8	R-12, R-22	161-1533
Shah [24]	7-40	R-11,R-12,R-22,R-113,methanol,ethanol benzene,toluene,trichloroethylene	11-211
Moser *et al.* [25]	3.14-20	R-11,R-12,R-22,R-125,R-134a,R-410a	-
Soliman [26]	7.4-11.66	Steam,R-12,R-113	80-1610
Dobson and Chato [27]	4.6, 7.04, 31.4	R-12,R-22,R-134a, R-32/R-125 (mix)	25-800
Koyama *et al.* [28]	0.807-1.062	R-134a	100-700

The pressure drop due to contraction is calculated by Eqn. (4):

$$\Delta p_i = \frac{1}{2} K \rho_g \left(\frac{\dot{m}}{\rho_g A_{mani}} \right)^2 \tag{4}$$

where K, ρ_g, $\dot{m}$, A_{mani}, are the friction coefficient (equal to 0.5), vapor density ($kg.m^{-3}$), mass flow rate ($kg.s^{-1}$) and manifold area (m^2), respectively.

The expansion pressure gain is calculated by the separated flow model, recommended by Hewitt *et al.* [16], as follows:

$$\Delta p_o = \frac{G^2 \gamma_{\exp} \left(1-\gamma_{\exp}\right) \psi_S}{\rho_l} \tag{5}$$

where

$$\psi_S = \left[1 + \left(\frac{\rho_l}{\rho_g} - 1 \right) \left(0.25x(1-x) + x^2 \right) \right] \tag{6}$$

$$\gamma_{\exp} = \frac{A_{tot,ch}}{A_{mani}} \tag{7}$$

where $A_{tot,ch}$ and A_{mani} are the internal area of all the channels and the manifold area.

The deceleration pressure gain is calculated using the model recommended by Carey [17]:

$$\Delta p_{de} = \left[\frac{G^2 x^2}{\rho_g \alpha} + \frac{G^2 (1-x)^2}{\rho_g (1-\alpha)} \right]_{X=X_{in}} - \left[\frac{G^2 x^2}{\rho_g \alpha} + \frac{G^2 (1-x)^2}{\rho_g (1-\alpha)} \right]_{X=X_{out}} \tag{8}$$

where α is the void fraction, which is calculated by Baroczy [18]:

$$\alpha = \left[1 + 0.28 \cdot \left(\frac{1-x}{x} \right)^{0.64} \cdot \left(\frac{\rho_g}{\rho_l} \right)^{0.36} \cdot \left(\frac{\mu_l}{\mu_g} \right)^{0.07} \right]^{-1} \tag{9}$$

Finally, we can calculate the two-phase friction pressure drop as follows:

$$\Delta p_o = \frac{1}{2} f_{tp} \frac{G^2 L}{\rho_l D} \tag{10}$$

where the two-phase friction factor, f_{tp}, can be correlated with liquid, liquid only, vapor and vapor only friction factors.

The experimental results for Δp are compared with the five correlations for which the references are furnished in Tab. 1.

Heat Transfer Coefficient

The experimental local convective condensation heat transfer coefficient, h, is defined as:

$$h(z)_{\exp} = \frac{\bar{q}''}{\bar{T}_{sat}(p(z)) - \bar{T}_w(z)} \tag{11}$$

where $\bar{q}''$, $\bar{T}_{sat}(p(z))$ and $\bar{T}_w$ represent the heat flux, the local saturation temperature and the wall temperature, respectively.

The heat flux is measured by the Peltier coolers, and the characteristic curves obtained experimentally are shown in Fig. 4. The local saturation temperature is a function of the local

Copyright © 2011 by ASME

pressure, which is determined by linear interpolation from the measurements of the pressure at the entrance and exit microchannels. The wall temperature is experimentally determined from the average of the readings taken at a particular location. The experimental results for h_{exp} are compared with the seven correlations for which the references are given in Tab. 2.

Uncertainty Analysis

The analysis of the uncertainties for the present experimental parameters, determined according to Holman [19] are summarized in Tab. 3.

TABLE 3. PARAMETERS AND RELEVANT ESTIMATED UNCERTAINTIES

Parameter	Uncertainty
Tube diameter, d	±4%
Surface area, A	±4%
Wall temperature, T_w	±0.3 K
Fluid temperature, T_f	±0.5 K
Pressure, p	±5 kPa
Pressure drop measured, ΔP_{exp}	±0.75 kPa
Mass velocity, G	±7%
Heat flux, q''	±3%
Experimental heat transfer coefficient, h	±12%

RESULTS

The results for the condensation in microchannels were obtained over a small range of conditions, for low mass velocity (G < 125 kg.m^{-2}s^{-1}).

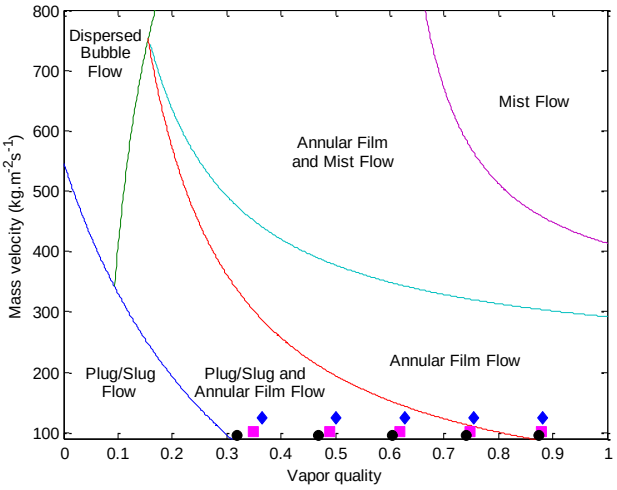

FIGURE 5. EXPERIMENTAL POINTS ON COLEMAN AND GARIMELLA [3] FLOW MAP

Fig. 5 shows the experimental points for G>95 kg.m^{-2}s^{-1} plotted on a Coleman and Garimella [3] flow map, developed for square tubes with D_h=1 mm. It can be observed that only a few experimental points lie within the annular film zone and the majority lie within the intermittent/annular region.

Heat Transfer Coefficient

Fig. 6 shows the heat transfer coefficients obtained at 13 different positions where the temperature was measured. The h_{exp} value decreased throughout the test section until z = 45 mm. This behavior is to be expected for condensation heat transfer, mainly for the annular pattern (high vapor qualities). This occurs because the annular film thickness increases with reducing x and the thermal resistance is greater for a heat flux in this pattern.

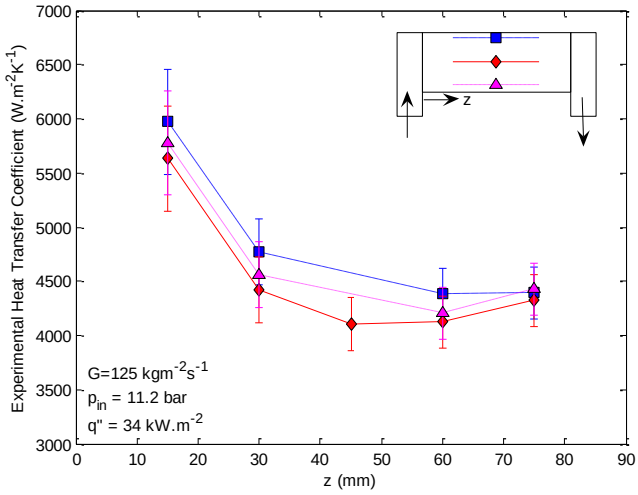

FIGURE 6. LOCAL EXPERIMENTAL CONDENSATION HEAT TRANSFER COEFFICIENTS AT DIFFERENT POINTS

According to Fig. 6, the last three locations show that the heat transfer coefficient tends to remain constant. This is to be expected because, for these locations, as shown in Fig. 5, the flow pattern changes to intermittent flow.

Fig. 7 shows the experimental data for the heat transfer coefficient as a function of x in the microchannels. These experimental data points were obtained by measuring the temperature in the five sections where the thermocouples are placed (see Fig. 3). For low qualities, h is independent of the mass velocity. The dependence of h on the vapor quality is not clear for x>0.6. It is important to note that, in these experiments, the fluid pressure is directly proportional to the mass velocity and, as discussed above, the heat transfer coefficient increases with the rise in pressure, and the opposite occurs due to the effect of G.

Copyright © 2011 by ASME

Fig. 8 presents the experimental heat transfer coefficients obtained in this study for under one set of conditions (the same as those related to the pink points in Fig. 7) compared with the seven correlations, cited in Tab. 2. The behaviors observed under the other test conditions are very similar to that observed in this study.

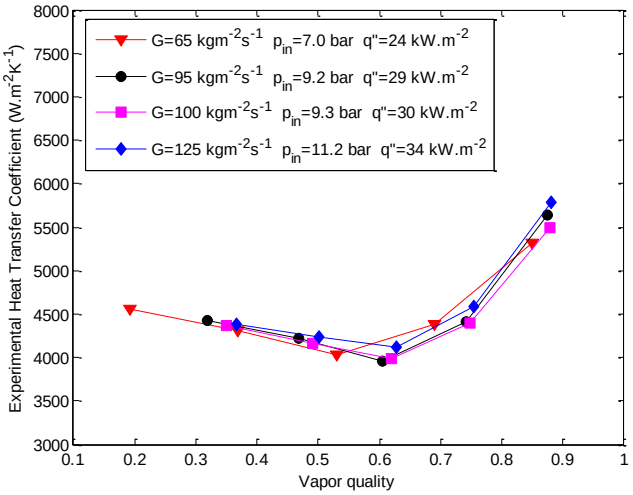

FIGURE 7. EFFECT OF MASS VELOCITY ON THE HEAT TRANSFER COEFFICIENT

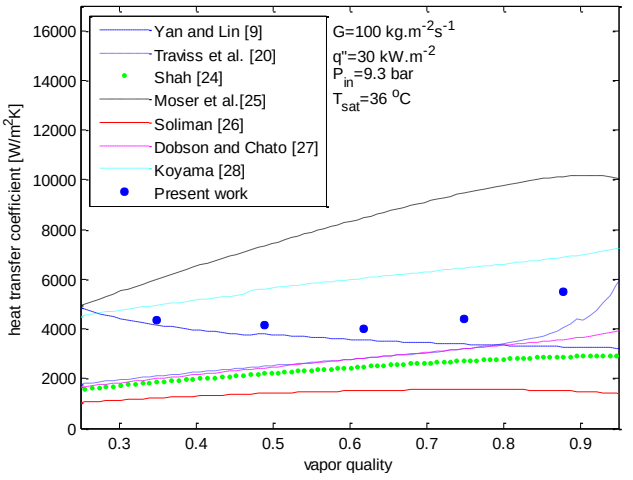

FIGURE 8. COMPARISON OF DIFFERENT CORRELATIONS AND EXPERIMENTAL VALUES FOR HEAT TRANSFER COEFFICIENT

According to Fig. 8, the correlation proposed by Yan and Lin [9] presents the best results, mainly for low qualities (x<0.7). For x>0.7 the behavior of the experimental results is different to that of this correlation. On analyzing the results in Fig. 8 together with those in the flow map in Fig. 5, it can be seen that the Yan and Lin [9] correlation fits well the data in the intermittent region (plug/slug), but not in the annular region.

Fig. 9 shows a comparison between the experimental results and the correlation proposed by Yan and Lin [9]. It confirms that this correlation does not provide a good fit only for larger vapor quality values. This good agreement (mean deviation of 18% for all data and 13% for x<0.8) can be explained by the fact that this correlation was developed for conditions very similar to those of the present study (see Tab. 2).

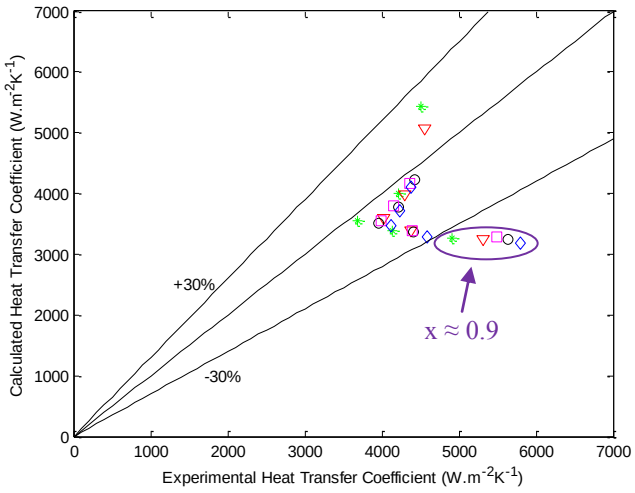

FIGURE 9. COMPARISON BETWEEN EXPERIMENTAL DATA AND YAN AND LIN [9] CORRELATION FOR HEAT TRANSFER COEFFICIENT

Pressure Drop

For the pressure drop four data points were obtained, which prevented a good experimental analysis of the influence of different parameters.

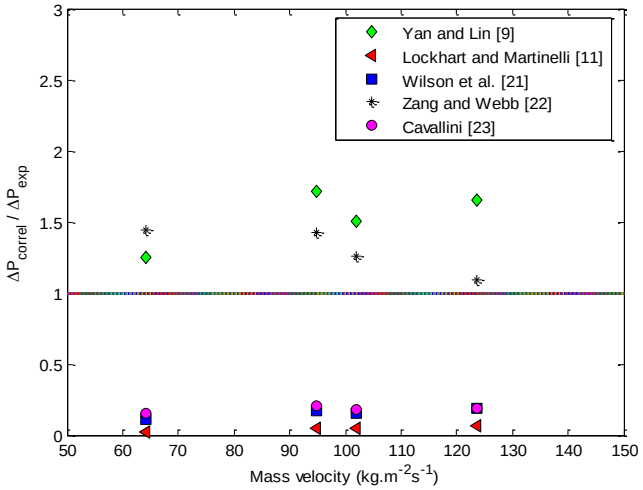

FIGURE 10. COMPARISON OF DIFFERENT CORRELATIONS AND EXPERIMENTAL VALUES FOR PRESSURE DROP

Copyright © 2011 by ASME

Fig. 10 shows a comparison of the experimental data with the different correlations proposed. Other correlations were tested but the results gave very small values, with deviations higher than 100% when compared with the experimental results.

The correlation that best fits the experimental data is that proposed by Zang and Webb [22], which gave a mean deviation of 30% compared with the experimental data. The mean deviation between the results calculated using the correlation of Yan and Lin [9] and the experimental data points was 53%.

CONCLUSIONS

The experimental characteristics of the pressure drop and heat transfer coefficient were investigated for the condensation of R-134a inside eight parallel microchannels with D = 0.8 mm. The following conclusions can be drawn from this study.

There was no clear effect of the mass velocity on the heat transfer coefficient for the range tested (65 to 125 $kg.m^{-2}s^{-1}$). The h value decreased with reducing vapor quality until $x \approx 0.60$, and became constant at lower values of x, indicating a change in the two-phase regime from annular to intermittent.

The correlation proposed by Yan and Lin [9] for the heat transfer coefficient gave the best results compared with the experimental data. For $x<0.9$ (intermittent region on the Coleman and Garimella [3] map) this correlation fits the experimental data very well, with a mean deviation of 13%.

For the pressure drop, five correlations were tested and that proposed by Zang and Webb [22] gave the best results, with a deviation of 30%.

ACKNOWLEDGMENTS

The authors are grateful for the support of CAPES and CNPq in the performance of this study. The experimental setup was financed by CNPq.

REFERENCES

[1] Matkovic, M., Cavallini, A., Del Col, D., and Rossetto, L., 2009, "Experimental study on condensation heat transfer inside a single circular minichannel," *International Journal of Heat and Mass Transfer*, **52** (9-10), pp. 2311-2323.

[2] Coleman, J. W., and Garimella, S., 1999, "Characterization of two- phase flow patterns in small diameter round and rectangular tubes, *International Journal of Heat and Mass Transfer*, **42**, pp. 2869-2881.

[3] Coleman, J.W., and Garimella, S., 2000, "Two-phase flow regime transitions in microchannel tubes: The effect of hydraulic diameter", *ASME HTD*, **366 (**4), pp. 71-83.

[4] Kim, M. H., Shin, J. S., Huh, C., Kim, T. J., and Seo, K. W., 2003, "A study of condensation heat transfer in a single mini-tube and review of korean micro- and mini-channel studies", *1st Int. Conf. on Microchannels and Minichannels*, Rochester, pp. 47–58.

[5] Kew, P., Cornwell, K., 1997, "Correlations for prediction of boiling heat transfer in small diameter channels", *Appl. Thermal Eng.*, **17**, pp. 705-715.

[6] Du, X.Z., Zhao, T.S., 2003, "Analysis of film condensation heat transfer inside a vertical micro tube with consideration of the meniscus draining effect", *International Journal of Heat and Mass Transfer*, **46** (24), pp. 4669- 4679.

[7] Ribatski, G., Wojtan, L., Thome, J.R., 2006, "An analysis of experimental data and prediction methods for two-phase frictional pressure drop and flow boiling heat transfer in micro-scale channels", *Experimental Thermal and Fluid Science*, **31**, pp. 1-19.

[8] Baird J., Fletcher, D.F., and Haynes, B.S., 2003, "Local condensation heat transfer rates in fine passages," *International Journal of Heat and Mass Transfer*, **46** (23), pp. 4453-4466.

[9] Yan Y.Y., Lin, T.F., 1999, "Condensation heat transfer and pressure drop of refrigerant R-134a in a small pipe", *International Journal of Heat and Mass Transfer*, **42**(4), pp. 697-708.

[10] Su Q., Yu G. X., Wang H. S., and Rose J. W. , 2009, "Microchannel condensation : Correlations and theory", *International Journal of Refrigeration*, **32**(6), pp. 1149-1152.

[11] Lockhart, R.W., Martinelli, R.C., 1949, "Proposed correlation of data for isothermal two-phase, two-component flow in pipes", *Chem. Eng. Prog.* pp. 39-48.

[12] Chisholm, D., 1973, "Pressure gradients due to friction during the flow of evaporating two-phase mixtures in smooth tubes and channels", *International Journal of Heat and Mass Transfer*, **16**, pp. 347–358.

[13] Friedel, L., 1979, "Improved frictional pressure drop correlations for horizontal and vertical two-phase pipe flow", In Eur. Two Phase Group Meeting, Ispra, Italy, Paper E2.

[14] Dalkilic A.S., and Wongwises S., 2009, "Intensive literature review of condensation inside smooth and enhanced tubes", *International Journal of Heat and Mass Transfer*, **52**(15-16), pp. 3409-3426.

[15] Garimella, S., 2005 "Condensation in Minichannels and Microchannels", In *Heat Transfer and Fluid Flow in Minichannels and Microchannels*, eds. S. G. Kandlikar, S. Garimella, D. Li, S. Colin, and M. King, Elsevier Publications, Oxford, UK..

[16] Hewitt, G. F., Shires, G. L., and Bott, T. R., 1993, *Process Heat Transfer*., Ed Ann Arbor, MI, CRC Press, Inc, pp. 402 & 410.

[17] Carey, V.P., 1992, "Liquid-vapor phase-change Phenomena, Hemi- sphere Publishing Corporation, New York, NY, February.

[18] Baroczy, C.J., 1965, "Correlation of liquid fraction in two-phase flow with application to liquid metals", *Chem. Eng. Progr. Sympos. Ser.*, **61** (57), pp. 179–191.

[19] Holman, J.P., 1989, "Experimental methods for engineering", 5th ed ., McGraw-Hill, New York.

 Copyright © 2011 by ASME

[20] Traviss, D.P., Rohsenow, W.M., Baron, A.B., 1973, "Forced-convection condensation inside tubes: a heat transfer equation for condenser design", *ASHRAE Trans.*, **79**, pp. 157–165.
[21] Wilson, M. J., Newell, T. A., Chato, J. C., and Infante Ferreira, C. A., 2003, "Refrigerant charge, pressure drop, and condensation heat transfer in flattened tubes", *Int. J. Refrig.*, **26**(4), 442–451.
[22] Zhang M., Webb, R.L., 2001, "Correlation of two-phase friction for refrigerants in small-diameter tubes", *Experimental Thermal and Fluid Science*, **25**(3-4), pp. 131-139.
[23] Cavallini, A., Censi, G., Del Col, D., Doretti, L., Longo, G. A., and Rossetto, L., 2002, "Condensation of halogenated refrigerants inside smooth tubes", *HVAC and R Research*, **8**(4), pp. 429–451.
[24] Shah, M.M., 1979, "A general correlation for heat transfer during film condensation inside pipes", *International Journal of Heat and Mass Transfer*, **22**, pp. 547-556.
[25] Moser, K.W., Webb , R.L., Na, B., 1998, "A new equivalent Reynolds number model for condensation in smooth tubes", *Journal of Heat Transfer*, **120**, pp. 410–417.
[26] Soliman, H.M., 1982, "On the annular-to-wavy flow pattern transition during condensation horizontal tubes", *Canadian Journal of Chemical Engineering*, **60**, pp. 475-481.
[27] Dobson, M.K., Chato, J.C., 1998, "Condensation in smooth horizontal tubes", *Journal of Heat Transfer*, **120**, pp. 193-213.
[28] Koyama, S., 2003, "An experimental study on condensation of refrigerant R134a in a multi-port extruded tube", *International Journal of Refrigeration*, **26**(4), pp. 425-432.

Copyright © 2011 by ASME